Interaction of a Fluorescent Derivative of Paclitaxel (Taxol)[1] with Microtubules and Tubulin−Colchicine[†]

Yi Han,[‡] A. G. Chaudhary,[§] M. D. Chordia,[§] D. L. Sackett,[∥] Bernardo Perez-Ramirez,[⊥] David G. I. Kingston,[§] and Susan Bane*,[‡]

Department of Chemistry, State University of New York at Binghamton, Binghamton, New York 13902-6016, Department of Chemistry, Virginia Polytechnic Institute and State University, Blacksburg, Virginia 24061-0212, Laboratory of Biochemical Pharmacology, NIDDK, NIH, Bethesda, Maryland 20892, and Graduate Department of Biochemistry, Brandeis University, Waltham, Massachusetts 02254-9110

Received April 1, 1996; Revised Manuscript Received August 14, 1996[⊗]

ABSTRACT: A fluorescent derivative of paclitaxel, 2-debenzoyl-2-(*m*-aminobenzoyl)paclitaxel (2-AB-PT), has been prepared. 2-AB-PT induces microtubule assembly *in vitro*, but is about 3-fold less potent than paclitaxel itself. The absorption and emission characteristics of 2-AB-PT were analyzed as a function of solvent. It was found that both spectra were perturbed by specific solvent effects when the solvent contained a hydrogen bond donor. The absorption and fluorescence spectra of 2-AB-PT bound to microtubules could not be mimicked by a single solvent, but the absorption and emission maxima of the tubulin-bound species could be duplicated by a solvent mixture of DMSO and water. These results indicate that the fluorophore binding site on the microtubule is in an environment of intermediate polarity that is accessible to a hydrogen bond donor in the vicinity of the *m*-amino group. In addition, tubulin fluorescence is quenched in the 2-AB-PT/microtubule complex, and energy transfer from tubulin to 2-AB-PT is apparent. These results indicate that substituents on the C-2 position of paclitaxel associate with tubulin when bound to the microtubule. 2-AB-PT binding to microtubules was quantitatively analyzed by fluorescence titrations. Two classes of binding sites for 2-AB-PT on microtubules were found. The high affinity site has an apparent association constant (K_{1app}) of 2.0 ($\pm$0.9) $\times$ 10^7 M^{-1} and an apparent binding stoichiometry (n_{1app}) of 0.8 ($\pm$0.1) sites/tubulin dimer in the microtubule. The apparent association constant for the lower affinity site is about 100-fold less than that of the higher affinity site (K_{2app} = 2.1 ($\pm$0.7) $\times$ 10^5 M^{-1}), and the stoichiometry of the lower affinity site or class of sites (n_{2app}) was found to be 1.3 $\pm$ 0.1. Paclitaxel blocked 2-AB-PT binding to the high affinity site. No binding of 2-AB-PT to unassembled tubulin was observed, but the emission spectrum of 2-AB-PT in the presence of the tubulin−colchicine complex resembled the emission spectrum of the ligand bound to microtubules. It was previously shown that paclitaxel can induce GTPase activity in the tubulin−colchicine complex, indicating that paclitaxel can bind to unassembled tubulin in its complex with colchicine [Carlier, M.-F., & Pantaloni, D. (1983) *Biochemistry 22*, 4814−4822]. Rigorous characterization of the aggregation state of the protein under these conditions demonstrates that 2-AB-PT is also capable of binding to the tubulin−colchicine complex.

Paclitaxel (Taxol),[1] a diterpene originally isolated from the bark of the Western Yew, *Taxus brevifolia*, has shown great utility in the treatment of certain human malignancies (Rowinski, 1992). Paclitaxel is a member of a diverse class of substances that inhibit cell division by interacting with tubulin or microtubules. Most antimicrotubule agents, such as colchicine, podophyllotoxin, combretastatin, the *Vinca* alkaloids, and related agents, inhibit *in vitro* tubulin assembly or depolymerize existing microtubules at micromolar concentrations (Hamel, 1990). Paclitaxel, however, affects the bulk properties of microtubules in a different fashion: paclitaxel promotes microtubule assembly and stabilizes microtubules against depolymerization, apparently through binding to a site on the microtubule rather than to soluble tubulin (Horwitz, 1992).

Recent studies indicate that the effect of antimicrotubule drugs on living cells may be mediated through modulation of microtubule dynamics rather than interference with the bulk properties of the microtubule (see, for example, Dhamodharan et al., 1995; Wilson & Jordan, 1995). At relatively low concentrations, vinblastine, colchicine bound to tubulin, and paclitaxel can kinetically stabilize microtubule dynamics without significantly changing the polymer mass. It may be that the mechanism by which antimicrotubule drugs kill cells is a result of this kinetic stabilization of the microtubules and not the action of the substances on the assembly and disassembly of the polymer (Wilson & Jordan, 1995).

The molecular mechanism(s) by which paclitaxel binds to and stabilizes microtubules is currently unclear. There are several characteristics of the paclitaxel−microtubule interaction that complicate the usual methods available for probing the ligand−receptor association. First, paclitaxel possesses no natural chromophore distinct from the chro-

[†] This work was supported in part by National Institutes of Health Grants CA55131 and CA48974 (to D.G.I.K.) and National Science Foundation Grant MCB9406424 (to S.B.). A preliminary account of this work has been presented (Han et al., 1994).

* Author to whom correspondence should be addressed.
[‡] State University of New York at Binghamton.
[§] Virginia Polytechnic Institute and State University.
[∥] NIDDK, NIH.
[⊥] Brandeis University.

[⊗] Abstract published in *Advance ACS Abstracts,* November 1, 1996.

[1] Taxol is a registered trademark of Bristol-Myers Squibb.

S0006-2960(96)00774-X CCC: $12.00

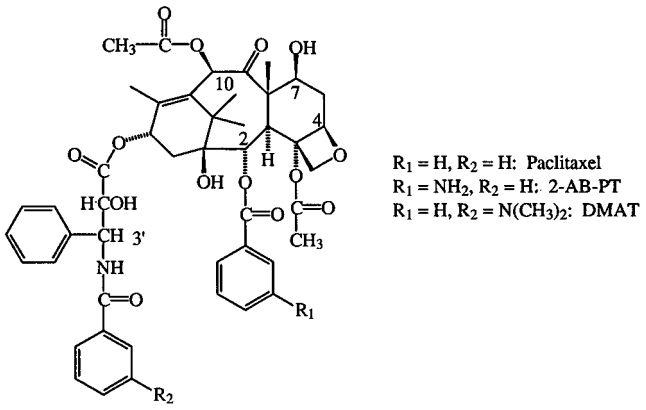

FIGURE 1: Structures of paclitaxel, 2-debenzoyl-2-(*m*-aminobenzoyl)paclitaxel (2-AB-PT), and *N*-debenzoyl-*N*-[3-(dimethylamino)-benzoyl]paclitaxel (DMAT).

mophoric regions of the protein. Changes that may occur in the electronic spectra of paclitaxel upon microtubule binding are obscured by the electronic spectra of the protein. Second, paclitaxel binds preferentially to microtubules rather than to tubulin (Parness & Horwitz, 1981; Ringel & Horwitz, 1991). The size of the receptor renders methods such as solution state NMR spectroscopy ineffectual. And third, the structural complexity of the molecule hampers synthetic efforts to create a broad spectrum of analogs for structure−activity studies. Structure−activity studies assist in defining the region(s) of the natural product necessary for high affinity binding to a receptor. This experimental approach may also guide the design of modified paclitaxels for mechanistic studies.

One approach to investigate the mechanism of paclitaxel binding to microtubules is to prepare a paclitaxel analog in which a fluorescent probe is covalently attached to the molecule (see, for example, Dubois et al., 1995; Souto et al., 1995). Sengupta et al. (1995) have recently prepared a fluorescent paclitaxel derivative in which the 3′-*N*-benzoyl group is replaced by a *m*-(dimethylamino)benzoyl group (DMAT;[2] Figure 1). This paclitaxel derivative retains high activity as a promoter of microtubule assembly *in vitro*. Moreover, it appears that this compound binds to unpolymerized tubulin. Specifically, fluorescence characteristic of DMAT bound to microtubules was observed in solutions of DMAT and tubulin under nonassembly conditions including low temperatures, the presence of podophyllotoxin, and the presence of urea. If this binding site is the same as the paclitaxel binding site on polymerized tubulin, which could not be precisely determined, current hypotheses about the mechanism by which paclitaxel induces tubulin assembly will need to be reconsidered.

We are preparing fluorescent paclitaxel derivatives to probe a variety of questions concerning the interaction of paclitaxel with tubulin and microtubules. In addition to mechanistic studies, these fluorescent paclitaxels can provide information concerning the nature of the paclitaxel binding site on microtubules and the location of this site relative to other tubulin-binding ligands. For our first fluorescent probe, we chose to replace the C-2 benzoyl substituent of paclitaxel with a *m*-aminobenzoyl group (2-AB-PT; Figure 1). It was hoped that such a minor modification of the parent molecule would not adversely affect the interaction of the analog with microtubules. Furthermore, it has been proposed that the substituent at the C-2 position of paclitaxel is in contact with the protein when paclitaxel is bound to the microtubule. An environmentally sensitive fluorescent probe, such as the aminobenzoyl group on 2-AB-PT, should be amenable to testing this hypothesis.

EXPERIMENTAL PROCEDURES

Materials. 2-Debenzoyl-2-(*m*-aminobenzoyl)paclitaxel (2-AB-PT) was prepared from paclitaxel by semisynthesis. 2′,7-Bis(triethylsilyl)-2-debenzoyl-2-(*m*-azidobenzoyl)paclitaxel was prepared as previously described (Chaudhary et al., 1994). Reduction of the azido group was achieved by hydrogenation on Pd/C, and 2-AB-PT was obtained after removal of the silyl protecting group using standard methanolic HCl conditions. The isolated material was homogeneous on TLC (hexane/ethyl acetate, 70:30) and had spectroscopic data consistent with its structure. The ^{1}H NMR spectrum of 2-AB-PT was essentially identical to that of paclitaxel except for the following resonances (the designations 2″, etc., refer to the protons of the aminobenzoyl ring): δ ($CDCl_3$) 2.49 (3H, s, 4-OAc), 3.81 (1H, d, H-3), 4.24 (1H, d, H-20a), 4.31 (1H, d, H-20b), 5.60 (1H, d, H-2), 6.85 (1H, H-4″), 7.23 (1H, H-5″), 7.60 (1H, H-2″). The peak for H-6″ was obscured under other aromatic proton signals. Paclitaxel was a gift of the late Matthew Suffness of the National Cancer Institute.

PIPES, EGTA, and GTP (type II-S) were obtained from Sigma. Quinine sulfate was obtained from Aldrich. Spectrograde solvents were used in absorption and fluorescence spectroscopy. The buffers used were as follows: PME buffer: 50 mM PIPES, 0.5 mM $MgSO_4$, 1 mM EGTA, pH 6.9; PMEG buffer: 100 mM PIPES, 1 mM $MgSO_4$, 2 mM EGTA, 0.1 mM GTP, pH 6.9; PMG buffer: 10 mM sodium phosphate, 16 mM $MgSO_4$, 0.1 mM GTP, pH 7.0.

Tubulin Purification and Protein Determination. Bovine brain tubulin, free of microtubule-associated proteins, was prepared by two cycles of assembly−disassembly followed by phosphocellulose chromatography (Williams & Lee, 1982) and stored in liquid nitrogen. Prior to use, the frozen pellets were gently thawed, centrifuged at 5000*g* for 10 min at 4 °C, and then desalted into the desired buffer on 1 mL Sephadex G-50 columns according to the method of Penefsky (1977). Tubulin concentrations were determined spectrophotometrically in PME buffer using $\epsilon_{278nm} = 1.23$ (mg/mL)$^{-1}$ cm^{-1} (Detrich & Williams, 1978). 2-AB-PT concentrations were determined spectrophotometrically using $\epsilon_{320nm} = 2.85 \times 10^3$ M^{-1} cm^{-1} in PME buffer containing 10% DMSO. Colchicine concentrations were also determined spectrophotometrically using $\epsilon_{352nm} = 1.69 \times 10^4$ M^{-1} cm^{-1} in PME buffer (Chabin et al., 1990).

Microtubule Assembly. Tubulin assembly was monitored using a Hewlett-Packard 8451A absorption spectrometer. Tubulin in PMG buffer was added to a prewarmed sample cell in the spectrometer, which was held at 37 °C using a

[2] Abbreviations: 2-AB-PT, 2-debenzoyl-2-(*m*-aminobenzoyl)paclitaxel; DMAT, *N*-debenzoyl-*N*-[3-(dimethylamino)benzoyl]paclitaxel; DMF, dimethylformamide; DMSO, dimethyl sulfoxide; EGTA, ethylene glycol bis(β-aminoethyl ether)-*N*,*N*,*N*′,*N*′-tetraacetic acid; GTP, guanosine 5′-triphosphate; PIPES, piperazine-*N*,*N*′-bis(2-ethanesulfonic acid); PC, personal computer; PME buffer, 50 mM PIPES, 0.5 mM $MgSO_4$, 1 mM EGTA, pH 6.9; PMEG buffer, 100 mM PIPES, 1 mM $MgSO_4$, 2 mM EGTA, 0.1 mM GTP, pH 6.9; PMG buffer, 10 mM sodium phosphate, 16 mM $MgSO_4$, 0.1 mM GTP, pH 7.0.

circulation water bath, and a baseline was recorded. Assembly was initiated by addition of paclitaxel or 2-AB-PT in DMSO followed by rapid mixing. We have found that, under these conditions, DMSO concentrations of ≤4% do not affect the rate or the extent of tubulin polymerization (data not shown). Thus, the concentration of DMSO was <4% in all samples. The polymerization process was followed by monitoring the increase in turbidity of the solution at either 350 nm (paclitaxel) or 400 nm (2-AB-PT), as 2-AB-PT has notable absorption at 350 nm.

Fluorescence Spectroscopy. Excitation and emission spectra were recorded on an SLM 8000 spectrofluorometer coupled to a PC. The appropriate temperature was maintained with a circulating ethylene glycol−water bath. A 2 × 10 mm quartz fluorescence cell was used and oriented such that the excitation beam passed through the smaller path. Excitation spectra were corrected for fluctuations in lamp intensity as a function of wavelength using a Rhodamine B solution in the reference channel of the instrument. Emission spectra were uncorrected. Appropriate background spectra were recorded and digitally subtracted from all presented spectra. The apparent emission spectrum of polymerized tubulin, which results from light scattering by the polymeric solution, was small relative to the microtubule-bound 2-AB-PT emission spectrum. Quantum yields of 2-AB-PT in solvents were determined by comparison to the quantum yield of quinine sulfate in 0.1 M sulfuric acid (Demas & Crosby, 1971). Microtubule-bound 2-AB-PT for quantum yield determination was prepared as described under Absorption Spectroscopy.

Absorption Spectroscopy. Absorption spectra were measured on a Hewlett-Packard Model 8451A diode array spectrometer at ambient temperature. The digitized data were transferred to a PC interfaced to the instrument. In order to calculate the Stokes shift of microtubule-bound 2-AB-PT, the absorption spectrum of 2-AB-PT bound to microtubules was required. Since microtubule-containing solutions are turbid, the apparent absorption due to light scattering needed to be removed from the absorption spectrum. This was accomplished in two different ways. First, the absorption spectrum of 2-AB-PT in the presence of 10-fold excess tubulin was recorded on a Perkin-Elmer Lambda 2 spectrophotometer equipped with a diffuse reflectance accessory. The experimental apparatus is routinely used for recording absorption spectra of turbid samples. Unfortunately, the monochrometer grating in the spectrophotometer produces an anomaly in the precise region of the absorption spectrum in which the absorption maximum of 2-AB-PT is found. Alternatively, the absorption spectrum of the microtubule-bound 2-AB-PT could be obtained using the Hewlett-Packard spectrometer, which contains a diode array detector and therefore no monochrometer anomalies.

Microtubule-bound 2-AB-PT was prepared by incubating 2-AB-PT (9 μM) with tubulin (90 μM) for 20 min at 37 °C to ensure complete binding of 2-AB-PT and a steady-state population of microtubules. A parallel sample containing paclitaxel (8 μM) and tubulin (90 μM) was prepared as a light-scattering reference. The absorbance of the solutions from 310 to 500 nm was measured and recorded. Five separate measurements of each spectrum were performed, and the spectra were digitally averaged. Since 2-AB-PT shows no absorbance at 500 nm, the entire averaged absorption spectra of the two samples were normalized at 500 nm to account for any differences in polymer mass in the solutions. The normalized spectrum of the paclitaxel−tubulin solution was then subtracted from the spectrum of the 2-AB-PT−tubulin solution. The resulting spectrum was virtually identical to the spectrum obtained using diffuse reflectance spectroscopy (without the grating anomaly), indicating that the method used on the diode array spectrometer was valid.

Competition of 2-AB-PT Binding to Microtubules or Tubulin−Colchicine by Paclitaxel. Tubulin (5 μM) or tubulin−colchicine (5 μM) was incubated with 2-AB-PT (5 μM) at 37 °C for 20 min. Fluorescence was monitored at the emission maximum of bound 2-AB-PT (430 nm; excitation wavelength = 320 nm). Paclitaxel in DMSO was then added into the mixture such that the final concentration of DMSO in the solution was <4%. The fluorescence spectrum due to unbound 2-AB-PT and scattering due to microtubules, which were small relative to the signal of the bound ligand, were digitally subtracted from the experimental spectrum. Fluorescence due to the added DMSO was negligible.

Preparation and Fluorescence Spectra of Tubulin−Colchicine and Tubulin−Colchicine/2-AB-PT. Tubulin (20 μM) was incubated with a 10-fold excess of colchicine at 37 °C for 30 min in PME buffer. Excess colchicine was removed by rapid gel filtration (Penefsky, 1977). Tubulin−colchicine/2-AB-PT was prepared by incubating 5 μM tubulin−colchicine with 5 μM 2-AB-PT at 20 °C for 20 min. Emission spectra (excitation wavelength = 320 nm) were recorded for all samples, and fluorescence due to tubulin-bound colchicine was subtracted from the tubulin−colchicine/2-AB-PT spectrum.

Measurement of 2-AB-PT Binding to Microtubules. Titration curves for 2-AB-PT binding to microtubules were constructed as follows. Samples were prepared by mixing tubulin (5 μM) in PMEG buffer containing DMSO with varying amounts of 2-AB-PT (0−40 μM) and were incubated at 37 °C for 30 min. The total concentration of DMSO in each solution was 4%. Absorption and fluorescence emission spectra (excitation wavelength = 330 nm) of each sample were measured after the incubation. The solutions were then centrifuged for 10 min at 90000*g* in a Beckman 42.2 Ti rotor at 23 °C to separate microtubules from the tubulin dimer and unbound ligand. The supernatants were carefully removed, and absorption and emission spectra (excitation wavelength = 330 nm) of the solutions were obtained. Additional samples containing tubulin in 10-fold excess over 2-AB-PT were treated in an identical fashion to obtain a fluorescence value for the fully bound 2-AB-PT.

The fluorescence data were analyzed in terms of two classes of independent binding sites by the equation:

$$r = n_1[\text{2-AB-PT}]_{\text{free}}/(K_{\text{d1,app}} + [\text{2-AB-PT}]_{\text{free}}) + n_2[\text{2-AB-PT}]_{\text{free}}/(K_{\text{d2,app}} + [\text{2-AB-PT}]_{\text{free}}) \quad (1)$$

where r is the binding function ($[\text{2-AB-PT}]_{\text{bound}}/[\text{MT}]_{\text{total}}$; $[\text{MT}]_{\text{total}}$ is the total concentration of tubulin in the form of microtubules in each sample), $K_{\text{d1,app}}$ and $K_{\text{d2,app}}$ are the apparent dissociation constants of the two classes of binding sites, and n_1 and n_2 are the apparent stoichiometries for each class of sites (mol of 2-AB-PT bound/mol of tubulin in microtubules). The concentration of free ligand in each sample was determined as follows: the emission intensity

at 430 nm of the supernatants (due to free ligand) was subtracted from the fluorescence of the original solutions at 430 nm (due to bound and free ligand) to yield fluorescence at 430 nm for microtubule-bound fluorescence, F_b. F_b was converted to $[2\text{-AB-PT}]_{bound}$ as follows: the fluorescence emission at 430 nm of 2-AB-PT/tubulin solutions in which the tubulin concentration was in 10-fold excess of the ligand concentration was measured. This value was divided by the concentration of 2-AB-PT in each sample to yield the fluorescence value per micromolar bound ligand ($F_{\mu M}$). The concentration of bound ligand was calculated at that point by $F_b/F_{\mu M}$. The concentration of free ligand was then determined by subtracting the concentration of bound ligand from the total ligand concentration for each sample. The concentration of tubulin in the form of microtubules in each sample was determined by finding the concentration of unassembled tubulin in the supernatants by absorption spectroscopy and subtracting this value from the total tubulin concentration. The absorption at 278 nm of these solutions was corrected for 2-AB-PT absorbance ($\epsilon_{278\ nm} = 2.66 \times 10^3\ M^{-1}\ cm^{-1}$ in PMEG buffer), which was usually small compared to protein absorbance. Finally, the binding function r was calculated for each sample by dividing the concentration of bound 2-AB-PT by the concentration of tubulin in microtubules.

The data r and $[2\text{-AB-PT}]_{free}$ were fit to eq 1 using the curve fitting software (Marquardt−Levenberg algorithm) in SigmaPlot 2.01 (Jandel Scientific). Initial guesses of the parameters were obtained from Scatchard plots of the data.

In order to determine if the two classes of binding site found for 2-AB-PT were also binding sites for paclitaxel, a second type of titration was performed. In this case, 30 μM paclitaxel was included in each solution. The samples were analyzed as above. In these samples, the concentration of microtubules was essentially equal to the total tubulin concentration and was constant for all samples. In this case, only a single hyperbola was required to fit the data, i.e.,

$$r = n[\text{2-AB-PT}]_{free}/(K_{d,app} + [\text{2-AB-PT}]_{free}) \qquad (2)$$

Electron Microscopy. Electron micrographs were obtained using a Hitachi 7000 TEM. Samples were analyzed on 200 mesh hydrophilic carbon-coated grids and were stained with uranyl acetate.

Analytical Ultracentrifugation. Sedimentation equilibrium experiments were performed at 10 °C with a Beckman Model E analytical ultracentrifuge. Runs were carried out in an An-F rotor using 12-mm Epon filled aluminum double-sector centerpieces and quartz windows. Short columns (50 μl of sample) and overspeeding were employed (Sackett & Lippoldt, 1991; Shearwin et al., 1994; Perez-Ramirez et al., 1994). Three cells, each containing a different initial concentration of protein, were used in each run. The concentration gradient in the cell was determined by UV absorbance at 276 nm using the photoelectric scanner and the standard Beckman multiplexer to separate the signals as previously described (Shearwin et al., 1994). Sedimentation data were analyzed by direct fitting of the concentration vs radial distance results to the basic sedimentation equation (Shire et al., 1991). A partial specific volume of 0.736 mL/mg was used for tubulin (Na & Timasheff, 1981). Solution density measurements were determined as previously described (Perez-Ramirez et al., 1994).

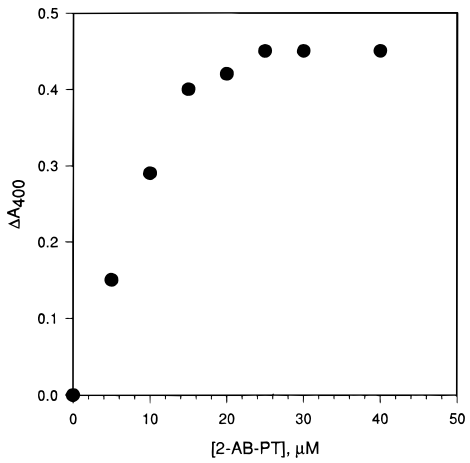

FIGURE 2: Extent of tubulin polymerization as a function of 2-AB-PT concentration. Tubulin (10 μM) in PMG buffer was assembled by the addition of varying concentrations of 2-AB-PT at 37 °C.

RESULTS

In Vitro Assembly of Microtubules Induced by 2-AB-PT. The fluorescent analog of paclitaxel employed in this study contained an aminobenzoate fluorophore at the 2-position of paclitaxel. The aminobenzoate chromophore may be constructed in three different isomeric forms. The anthranilate chromophore, in which the amino group is *ortho* to the ester, is the most commonly used isomer for probing biological systems (see, for example: Birmachu & Reed, 1988). Previous structure−activity studies at the C-2 position of paclitaxel have shown that substitution at the *meta* position can lead to highly active paclitaxel analogs (Chaudhary et al., 1994). Therefore, the *m*-aminobenzoate chromophore was chosen for this study.

Figure 2 shows the effect of 2-AB-PT on the assembly of pure tubulin into microtubules. The extent of tubulin assembly, as judged by the relative increase in turbidity of the solution, increases with increasing 2-AB-PT concentration up to a molar ratio of about 3:1 (2-AB-PT:tubulin). Electron micrographs of tubulin polymerized by 2-AB-PT showed normal microtubules (data not shown). Similar experiments with paclitaxel show that the extent of tubulin assembly increases with increasing paclitaxel concentration up to a maximum at 1:1 (paclitaxel:tubulin; Diaz & Andreu, 1993). This result shows that 2-AB-PT is less potent than paclitaxel in promoting tubulin assembly.

The critical concentrations for microtubule formation were determined in PMG buffer in the presence of either 20 μM 2-AB-PT or 20 μM paclitaxel to be 1.5 ± 0.6 μM tubulin and 0.3 ± 0.1 μM tubulin, respectively (data not shown). Thus, addition of an amino group *meta* to the ester decreases the potency of the analog in this assay by about a factor of 5.

Fluorescent Properties of 2-AB-PT. The aminobenzoate chromophore has been used as a small, solvent sensitive fluorescent probe in a number of biological systems (Birmachu & Reed, 1988; Thulborn & Sawyer, 1978). Solvent-dependent changes in emission spectra can be a useful tool for determining the environment of a receptor-bound fluorophore (see, for example: Lakowicz, 1983). Interpretation of the spectra shifts must be done with care, however, as the spectral shifts may not be a simple function of the dielectric properties of the fluorophore's environment.

Table 1: Absorption and Fluorescence Properties of 2-AB-PT

solvent	$E_T(30)^a$	A_{max} (nm)^b	em_{max} (nm)^c	$(\nu_a - \nu_f) \times 10^{-3}$ (cm^{-1})
dioxane	36.0	328	398	5.5
ethyl acetate	38.1	328	404	5.7
dmf	43.8	334	420	6.2
dmso	45.0	336	430	6.5
2-propanol	48.6	328	444	8.0
ethanol	51.9	326	446	8.3
methanol	55.0	326	446	8.3
2% DMSO/water	63.1	320	454	9.3
microtubules		334	430	6.7
10% water/DMSO		334	430	6.7

[a] $E_T(30)$ is an empirical solvent polarity parameter. Values for $E_T(30)$ from Dimroth et al. (1963). [b] Absorption maximum. [c] Emission maximum

Analysis of the absorption and emission spectra of aminobenzoates as a function of solvent show that these fluorophores are subject to interactions with solvent that affect the dipole moment of the ground and excited states. Specifically, the absorption and emission spectra of the aminobenzoate fluorophores can be affected by hydrogen bond donating and hydrogen bond accepting solvents (Mataga, 1963). The anthranilate fluorophore (*ortho* isomer) is less affected by solvent interactions due to the presence of intramolecular hydrogen bonding between the amino and carbonyl groups. The *meta* isomer, however, contains no intramolecular hydrogen bonding and so is more strongly affected by specific solvent interactions. Structure−activity and synthetic considerations impelled us to use the *meta* isomer for this study. It was therefore important to examine the photochemical properties of 2-AB-PT in the absence of microtubules.

The absorption and emission properties of 2-AB-PT as a function of solvent are shown in Table 1. In aprotic solvents (dioxane−DMSO), the absorption maximum undergoes a blue shift with decreasing solvent polarity, while in protic solvents (2-propanol−water), the absorption maximum undergoes a red shift with decreasing solvent polarity. These data clearly show that a hydrogen bonding interaction exists between the ground state of the fluorophore and protic solvents. The nature of the excited state of the fluorophore can be examined by evaluating the relationship between solvent properties and the Stokes shift (Lippert, 1957; Mataga et al., 1956). Figure 3 shows that the Stokes shift is not a linear function of solvent polarity, demonstrating that the photochemical properties of the probe cannot be fully described by general solvent effects. Deviations from linearity occur in protic solvents such as water and alcohols, which are capable of donating a hydrogen bond to the fluorophore. Thus, the fluorophore on 2-AB-PT is subject to specific solvent effects in both the ground and excited states, and the existence of these specific solvent effects must be taken into consideration in the interpretation of the spectral shift of the microtubule-bound fluorophore.

The absorption and emission spectra for 2-AB-PT bound to microtubules are shown in Figure 4. The quantum yield of 2-AB-PT in buffer (0.006) increased to 0.15 upon microtubule binding, and a blue shift in the emission spectrum occurred. The absorption maximum of microtubule-bound 2-AB-PT (Table 1) suggests that the binding site polarity is near that of DMF, which is significantly red-shifted relative to the spectrum in water. The emission maximum of 2-AB-PT bound to the microtubule, however,

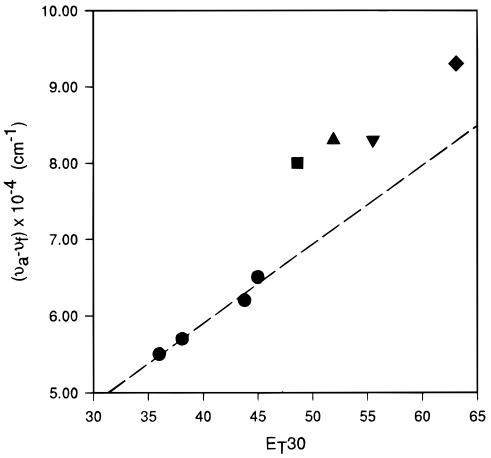

FIGURE 3: Stokes shifts of 2-AB-PT as a function of solvent polarity. Data for this plot were taken from Table 1. Symbols: circles, non-hydrogen bond donors; square, 2-propanol; triangle, ethanol; inverted triangle, methanol; diamond, 2% DMSO/water. The dashed line was calculated by linear regression analysis of the non-hydrogen bond donor data.

is at lower energy than the emission maximum of the probe in DMF. Hence, the binding site environment of 2-AB-PT cannot be adequately described by simple solvent effects or mimicked by a single solvent.

The absorption and emission spectra of 2-AB-PT were therefore examined in a mixture of an aprotic solvent (DMSO) and water (Figure 5). When the concentration of water in DMSO is ≥10%, a linear relationship is found between the Stokes shift and the solvent composition. At these higher water concentrations, the specific solvent effects on the fluorophore are saturated. These data can then be used to evaluate the nature of the fluorophore binding site. The Stokes shift of 2-AB-PT bound to microtubules is mimicked by the water/DMSO system at a water concentration of about 10% (Table 1). We therefore conclude that the polarity of the fluorophore binding site for 2-AB-PT on microtubules is similar to the polarity of DMSO but that the fluorophore is exposed to hydrogen bond donor(s) when bound to microtubules.

Energy transfer from tubulin to 2-AB-PT is observed in both the excitation (Figure 6A) and emission (Figure 6B) spectra of the microtubule-bound 2-AB-PT. Unliganded 2-AB-PT and paclitaxel-induced microtubules show little apparent emission at 450 nm when excited in the region of 280 nm (Figure 6A). Emission at 450 nm is observed from the protein excitation band when 2-AB-PT is bound to microtubules, indicating that the observed band in the complex is due to energy transfer from the protein to 2-AB-PT. When the sample is excited in the protein band, emission due to protein chromophores is decreased with 2-AB-PT binding and emission intensity due to 2-AB-PT is observed (Figure 6B). These observations further show that the fluorophore on 2-AB-PT is associated with the protein.

Direct Measurement of 2-AB-PT Binding to Microtubules. The binding of 2-AB-PT to microtubules is inhibited by excess paclitaxel, suggesting that 2-AB-PT binds to the same site as paclitaxel on microtubules (Figure 7). The fluorescence intensity of 2-AB-PT due to microtubule binding was decreased by up to 80% in the presence of paclitaxel under our experimental conditions.

The presence of bound ligand fluorescence in Figure 7 indicated that 2-AB-PT may be binding to additional protein

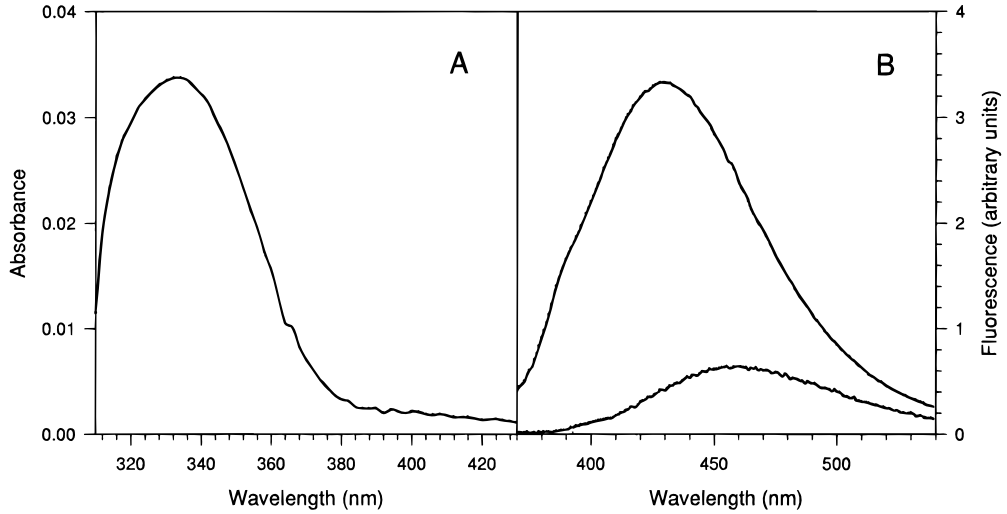

FIGURE 4: Absorption (A) and emission (B) spectra of 2-AB-PT bound to microtubules. Microtubule-bound 2-AB-PT was prepared by incubating 9 μM with 90 μM tubulin in PMEG buffer for 20 min at 37 °C prior to the measurement. Appropriate backgrounds were digitally subtracted from all spectra. Panel A: The absorption spectrum was determined as described under Experimental Procedures. Panel B: The upper curve is the emission spectrum of microtubule-bound 2-AB-PT. The lower curve is the emission spectrum of 54 μM 2-AB-PT in PMEG buffer containing 2% DMSO, which is shown to illustrate the increase in emission intensity and energy of 2-AB-PT upon microtubule binding. The excitation wavelength was 320 nm, and spectra were recorded at 37 °C.

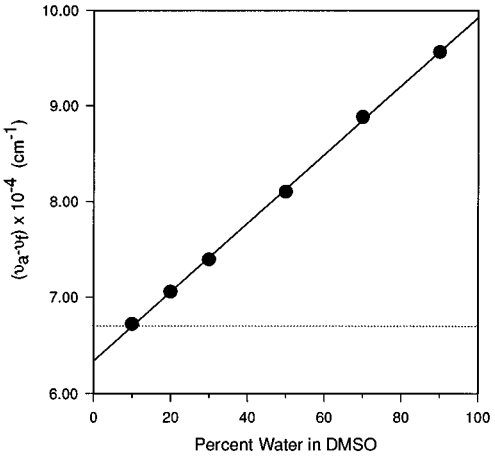

FIGURE 5: Effect of solvent composition on Stokes shifts of 2-AB-PT. The absorption and emission maxima of 2-AB-PT (11 μM) were determined in DMSO solutions containing water. The Stokes shift was a linear function of solvent composition at water concentrations of ≥10% (solid line), indicating that the specific solvent effect of water on the fluorophore is saturated at these concentrations. The dotted line shows the Stokes shift of microtubule-bound 2-AB-PT. The environment of the microtubule-bound fluorophore can be estimated from the intersection of the two lines.

species in solution. To determine if the fluorescence in the presence of saturating amounts of paclitaxel was due to 2-AB-PT binding to unassembled tubulin dimer, emission spectra of a solution containing 5 μM tubulin, 5 μM 2-AB-PT, and 30 μM paclitaxel in PMEG buffer were measured before and after centrifugation to pellet the microtubules (i.e., 90 000*g* for 10 min at 23 °C; it was found that 5 μM tubulin dimer does not pellet under these centrifugation conditions). The emission spectrum of the solution prior to centrifugation (excitation wavelength = 330 nm) had a maximum characteristic of microtubule-bound 2-AB-PT (432 nm). The emission spectrum of the supernatant had a broad maximum around 453 nm, which is characteristic of unbound ligand. No microtubules or other structures were seen in an electron micrograph of the supernatant (data not shown). It therefore appeared that the fluorescence emission observed at saturating concentrations of paclitaxel was not due to 2-AB-PT binding to the soluble tubulin dimer.

The association of 2-AB-PT with microtubules was therefore investigated by fluorescence titration as described u*nder Experimental Procedures.* A binding curve was constructed (Figure 8A), and a Scatchard plot of these data indicated that at least two classes of binding site were present on the microtubule for 2-AB-PT (inset, Figure 8A). Nonlinear regression analysis of the binding curve according to eq 1 yielded the parameters for the two classes of binding sites. The high affinity site has an apparent association constant (K_{1app}) of 2.0 (±0.9) × 10^7 M^{-1} and an apparent binding stoichiometry (n_{1app}) of 0.8 (±0.1) sites/tubulin dimer in the microtubule. The dissociation constant for 2-AB-PT binding to the high affinity site is about a factor of 3 greater than the dissociation constant determined by Caplow et al. (1994) for paclitaxel binding to GTP microtubules ($K_d \cong$ 15 nM vs $K_{d1,app}$ = 50 nM for 2-AB-PT). The apparent association constant for the lower affinity site is about 100-fold less than that of the higher affinity site (K_{2app} = 2.1 (±0.7) × 10^5 M^{-1}), and the stoichiometry of the lower affinity site or class of sites (n_{2app}) was found to be 1.3 ± 0.1. A better estimate of the parameters for the second site(s) could be obtained using higher concentrations of 2-AB-PT, but ligand solubility limited the concentration range that could be employed for these experiments.

In order to determine if paclitaxel shares the two types of bindings sites found for 2-AB-PT, a second binding curve was constructed in which each sample contained a 6-fold excess of paclitaxel relative to the tubulin concentration (i.e., 30 μM paclitaxel and 5 μM tubulin). These data (Figure 8B) could be fit assuming a single class of binding sites with an apparent association constant of 6.9 (±1.7) × 10^4 M^{-1} and a stoichiometry of 0.8 (± 0.1) mol of 2-AB-PT bound/mol of tubulin in microtubules.

Binding of 2-AB-PT to the Tubulin−Colchicine Complex. During preliminary examination of the excitation and emission properties of 2-AB-PT in the presence of tubulin, we observed fluorescence spectra characteristic of microtubule-bound 2-AB-PT at low (2 μM) tubulin concentrations. No

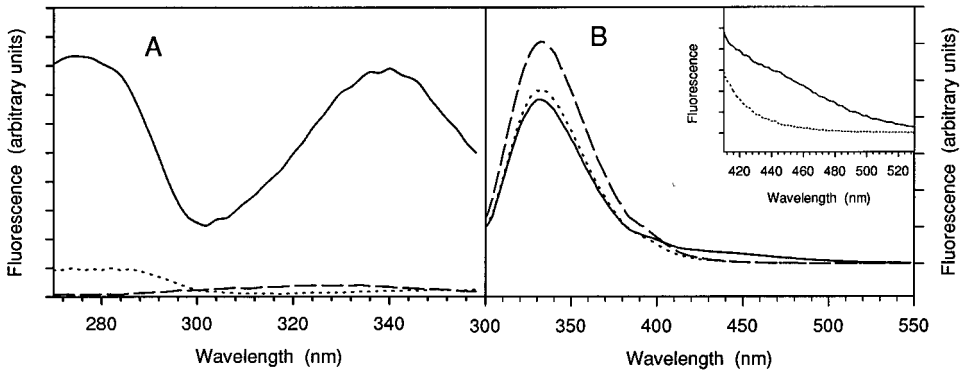

FIGURE 6: Panel A: Excitation spectra of 2-AB-PT in buffer (dashed curve), and of 2-AB-PT bound to microtubules (solid curve) and paclitaxel-induced microtubules (dotted curve). Polymerized tubulin was formed by incubating tubulin (10 μM) with 2-AB-PT (30 μM) or with paclitaxel (20 μM) at 37 °C prior to recording the spectra at 37 °C. The emission wavelength was 450 nm, and appropriate background spectra were digitally subtracted from the experimental data. Panel B: Effect of polymerization and of 2-AB-PT binding on the emission spectrum of tubulin. Samples were prepared by incubating tubulin (10 μM) without drug or with 2-AB-PT (30 μM) or paclitaxel (20 μM) for 20 min at 37 °C. Emission spectra of tubulin (dashed curve), paclitaxel-induced microtubules (dotted curve), and 2-AB-PT-induced microtubules (solid curve) were recorded at 37 °C (excitation wavelength = 290 nm). Inset: The region from 410 to 530 nm of 2-AB-PT-induced microtubules (solid curve) and paclitaxel-induced microtubules (dotted curve), enlarged to show the apparent energy transfer from tubulin to microtubule-bound 2-AB-PT.

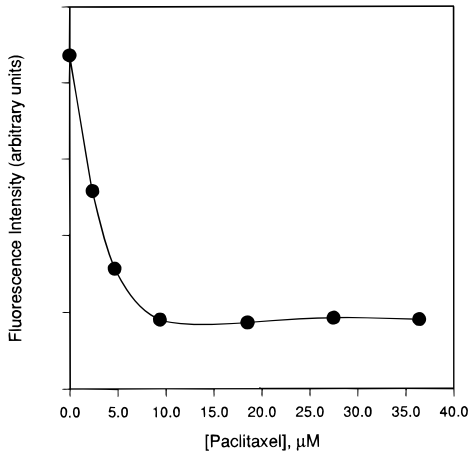

FIGURE 7: Inhibition of 2-AB-PT binding to microtubules by paclitaxel. Microtubule-bound 2-AB-PT was prepared by incubating tubulin (5 μM) with 2-AB-PT (5 μM) at 37 °C for 20 min in PMEG buffer. The emission intensity of 2-AB-PT (excitation wavelength = 320 nm, emission wavelength = 440 nm) was measured in samples containing varying amounts of paclitaxel at 37 °C.

turbidity of the solution was seen by light scattering in the absorption spectrophotometer under these conditions. Electron micrographs of the sample, however, showed the presence of a few small microtubules. When microtubules formed with 2-AB-PT were separated from unassembled protein by ultracentrifugation, the emission spectrum of the supernatant displayed a maximum near 453 nm, which is characteristic of unbound 2-AB-PT. Thus, under our experimental conditions, we found no evidence for 2-AB-PT binding to the unassembled tubulin dimer.

It has been shown previously that paclitaxel enhances tubulin GTPase activity induced by colchicine (Carlier & Pantaloni, 1983). These results were interpreted to demonstrate that paclitaxel binds to the unpolymerized tubulin−colchicine complex. In Figure 9 it is shown that the emission spectrum of 2-AB-PT increases in intensity and shifts to higher energy (near 430 nm) in the presence of the tubulin−colchicine complex. No turbidity of the solution could be observed by absorption spectroscopy, and an electron micrograph of the solution showed no microtubules or other structures (data not shown). Attempts to displace 2-AB-PT with paclitaxel in this system, however, were unsuccessful at paclitaxel concentrations up to 50 μM.

Electron microscopy can be used to observe microtubules, protofilaments, rings, and other larger aggregates of tubulin, but the absence of these structures in the fixed sample does not necessarily demonstrate that the original sample was free of aggregates. We therefore examined the aggregation state of tubulin−colchicine in the presence of 2-AB-PT or of 2-AB-PT and paclitaxel by sedimentation equilibrium analysis. The sedimentation equilibrium profiles obtained are shown in Figure 10. Molecular weight (M_{app}) values for tubulin−colchicine in the presence of either 2-AB-PT or a combination of 2-AB-PT and paclitaxel, derived from the close fits to the basic sedimentation equation (Shire et al., 1991), indicated that the protein under both conditions remains as a dimer in the protein concentration range of 0.1−5.0 μM. The equilibrium sedimentation data show no evidence for minor populations of oligomeric species other than the dimer of 110 000 ± 800 daltons. Sedimentation equilibrium analysis at lower rotor speed (18 000 rpm for 30 min and 15 000 rpm for 90 min) did not show the presence of aggregated protein (data not shown).

DISCUSSION

Binding of 2-AB-PT to Microtubules. The fluorescent analog of paclitaxel, 2-AB-PT, has been shown to induce the assembly of tubulin into microtubules (Figure 2). 2-AB-PT was 3- to 5-fold less potent than paclitaxel as an inducer of tubulin assembly. Structure-activity studies of 2-substituted benzoyl analogs have shown that the activity of paclitaxel analogs is quite sensitive to the nature of the substituent at C-2 (Chaudhary et al., 1994; Chen et al., 1994; Georg et al., 1995), so the small difference in activity is not surprising. Microtubule binding induced a blue shift in the emission spectrum of 2-AB-PT and a 25-fold increase in the quantum yield of the molecule, which rendered 2-AB-PT a valuable probe for fluorescence analysis of the ligand−microtubule interaction.

2-AB-PT bound to microtubules was displaced by paclitaxel, but about 20% of the initial fluorescence intensity (corrected for unbound drug) remained at saturating con-

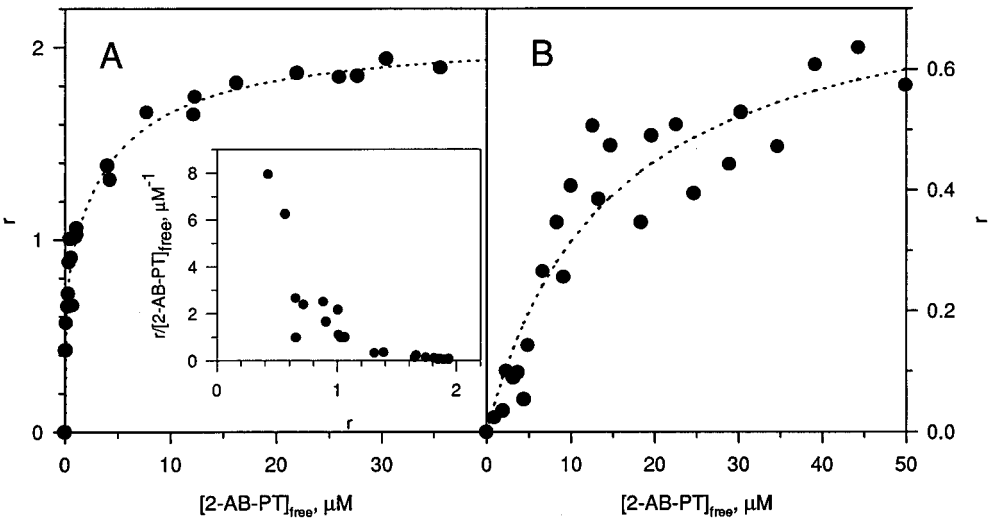

FIGURE 8: Binding of 2-AB-PT to microtubules in the absence (A) and presence (B) of 30 μM paclitaxel. Both titration curves were constructed and analyzed as described under Experimental Procedures. The dotted lines are the best fit to the data. Panel A: Tubulin (5 μM) was titrated with varying amounts of 2-AB-PT (0−47 μM). Inset: Scatchard plot of the data indicates the presence of at least two types of binding sites. Panel B: Tubulin (5 μM) was titrated with varying amounts of 2-AB-PT (0 - 52 μM) in the presence of 30 μM paclitaxel.

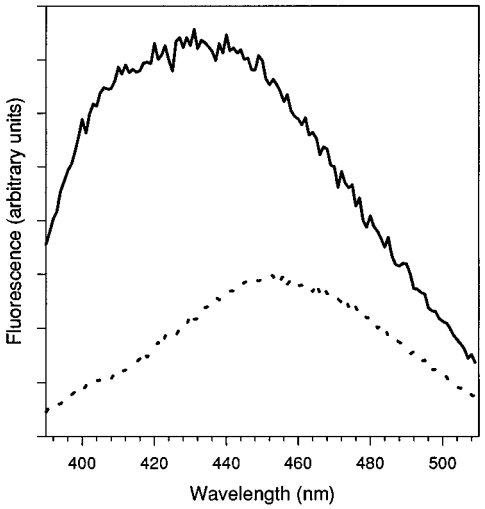

FIGURE 9: Fluorescence emission spectrum of 2-AB-PT (5 μM) in the presence (solid curve) and absence (dotted curve) of the tubulin−colchicine complex (5 μM) in PME buffer. The excitation wavelength was 320 nm, and the spectra were recorded at 20 °C. Fluorescence emission due to tubulin-bound colchicine was digitally subtracted from the spectrum of 2-AB-PT in the presence of the tubulin−colchicine complex.

centrations of paclitaxel (Figure 7). This observation implied that the fluorescent paclitaxel does bind to the paclitaxel site on microtubules but may also associate with other protein species in the solution. We found that the "excess fluorescence" was not due to 2-AB-PT binding to unassembled tubulin, implying that the fluorophore may be binding to an additional site(s) on the microtubule.

The association of 2-AB-PT with microtubules was therefore explored using fluorescence spectroscopy. Through fluorescent titrations, we found evidence for a high affinity site for 2-AB-PT, which we assign as the paclitaxel binding site. The apparent affinity constant of 2-AB-PT for the higher affinity site was about a factor of 3 less than the affinity constant for paclitaxel binding to microtubules, which corresponds to differences in the extent of polymerization as a function of drug concentration (Figure 2). Furthermore, when the paclitaxel binding site was saturated with paclitaxel, this high affinity site was no longer observable in the fluorescence titration (Figure 8B).

We were quite surprised to detect a second class of binding sites on the microtubule for 2-AB-PT. The apparent affinity constant for 2-AB-PT binding to this site(s) was found to be about 100-fold less than the apparent affinity of 2-AB-PT for the high affinity site. We attempted to characterize this binding site by measuring the association of 2-AB-PT to microtubules in which the paclitaxel binding site was fully occupied. There was a small decrease in the apparent association constant for 2-AB-PT to the second class of site(s) in the presence of excess paclitaxel (by a factor of about 3), and the apparent number of binding sites for 2-AB-PT was also reduced (from 1.3 to 0.8). It must be noted, however, that the parameters for 2-AB-PT binding to the low affinity site(s) were determined from data collected under conditions in which this binding site is not saturated, so the differences in the binding parameters in the presence and absence of paclitaxel may not be significant. Saturation conditions in these experiments cannot be obtained with 2-AB-PT due to its low solubility in aqueous solution. We are therefore reluctant to propose whether or not the low affinity site for 2-AB-PT is also a binding site for paclitaxel.

We therefore conclude that 2-AB-PT binds to the paclitaxel site on microtubules and that the affinity of paclitaxel for the binding site is slightly decreased by the addition of an amino group at the *meta* position of the C-2 benzoyl substituent. A second, lower affinity class of binding sites on the microtubule for 2-AB-PT is also present, but the physical significance of this site is unclear. A fluorescent paclitaxel derivative with higher water solubility will be necessary to evaluate the low affinity class of sites.

Spectroscopic Analysis of 2-AB-PT Bound to Microtubules. Steady-state fluorescence spectra of 2-AB-PT bound to microtubules were obtained under conditions in which a negligible amount of 2-AB-PT was bound to the low affinity site(s) on the microtubule. This discussion therefore pertains to the high affinity binding site shared with paclitaxel.

The absorption and fluorescence spectra of the microtubule-bound 2-AB-PT clearly demonstrate that the fluorophore

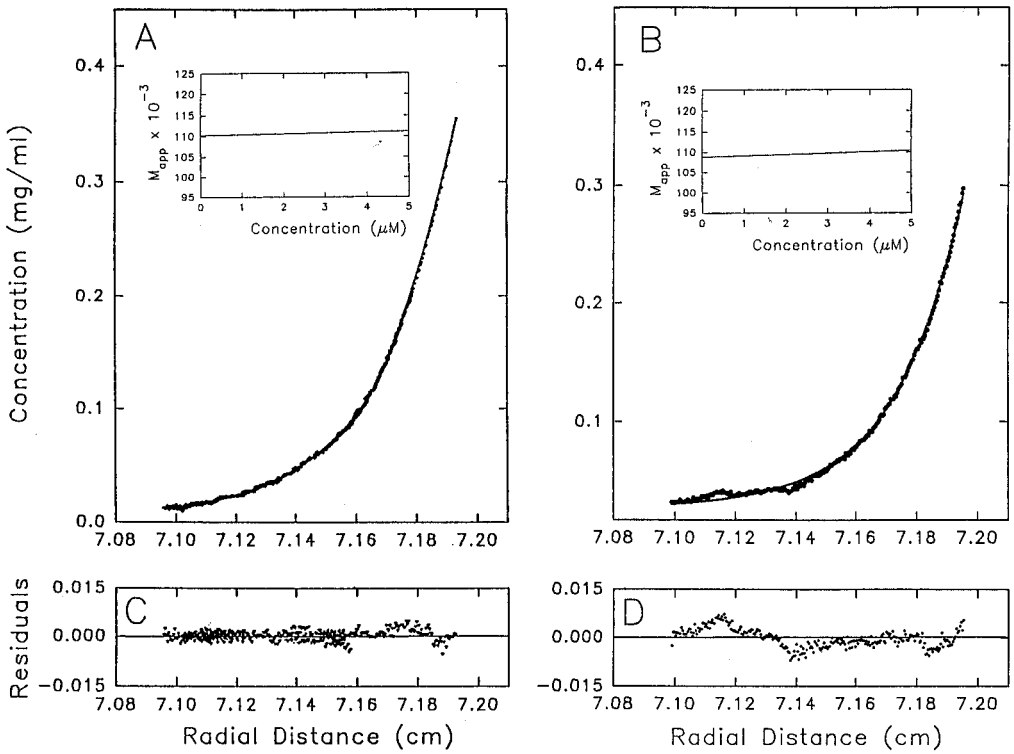

FIGURE 10: Sedimentation equilibrium of (A) tubulin−colchicine (5 μM) containing 5 μM 2-AB-PT and (B) tubulin−colchicine (5 μM) containing 5 μM 2-AB-PT and 50 μM paclitaxel in PME buffer. Samples (50 μL) were run in double sector cells in an An-F rotor for 60 min at 28 000 rpm, followed by 60 min. at 22 000 rpm at 10 °C. The concentration gradient in the cell was determined by ultraviolet absorption at 276 nm. The dots represent the experimental data (~250 points across the 1 mm column), while the solid lines show the best fit to the data (see Experimental Procedures). Insets are the apparent molecular weights in function of protein concentration. Panels C and D are plots of the differences between the experimental data and the data calculated from the fitted values.

is in contact with the protein, as predicted by structure−activity studies and inferred from molecular modeling. NMR and molecular modeling studies of paclitaxel in solution favor a "hydrophobic clustering" of the 2-benzoyl, 3′-phenyl, and 4-acetyl groups that may "preorganize" paclitaxel into an active conformation for binding to microtubules (see, for example: Dubois et al., 1993; Williams et al., 1993; Vander Velde et al., 1993). These studies and structure−activity investigations would seem to imply an overall hydrophobic environment for the 2-benzoyl portion of the molecule. Interestingly, the spectroscopic studies in this work indicate that the binding site environment of the *m*-aminobenzoyl group of 2-AB-PT is not purely hydrophobic, as might be expected for a binding site that accommodates an aromatic ring. For example, allocolchicine is a biaryl ligand that binds to the colchicine site on tubulin. The colchicine binding site was estimated from solvent studies of allocolchicine fluorescence to be quite apolar (near the polarity of dioxane and ethyl acetate; Hastie, 1989). In contrast, our spectroscopic analyses indicate that the binding site environment for the fluorophore of 2-AB-PT is relatively polar (dielectric constant near that of DMSO) and furthermore is accessible to or contains a hydrogen bond donor in the vicinity of the *m*-amino group. The spectroscopic data presented here cannot be used to distinguish between a hydrogen bond donor on the exterior and the interior of the binding site. However, it is difficult to see, based on current models of the 3-D structure of paclitaxel, how a hydrogen bond could be donated to the *m*-amino group by external water. Thus, although the origin of the hydrogen bond donor to the *m*-amino group is unknown, clear spectroscopic evidence for its existence has been found.

The excitation and emission spectra of 2-AB-PT bound to microtubules show the presence of energy transfer from tubulin to 2-AB-PT, indicating that at least one of the eight tryptophan residues of tubulin is in the vicinity of the paclitaxel binding site. More detailed information about the possible involvement of tryptophan residue(s) in 2-AB-PT binding to microtubules cannot be ascertained from these data, but more insight into a potential relationship between tubulin tryptophan residues and the paclitaxel binding site may be accessible through measurements of tryptophan emission decay kinetics in the presence and absence of 2-AB-PT (Cheung, 1991).

2-AB-PT Binding to the Tubulin−Colchicine Complex. Prior to the report of Sengupta et al. (1995), experimental data showed that paclitaxel binds to assembled microtubules but not to tubulin in its dimeric state. This constraint led to the proposal of an elegant thermodynamic model for paclitaxel-induced tubulin assembly in which paclitaxel binding to microtubules without binding to unpolymerized tubulin leads to enhanced tubulin assembly (Diaz & Andreu, 1993). The fluorescent paclitaxel analog DMAT, however, was clearly shown to interact with tubulin under nonassembly conditions. These findings indicate that a thermodynamic model for paclitaxel-induced tubulin assembly in which paclitaxel first binds to tubulin, similar to the model for the *Vinca* alkaloids binding to tubulin (for a review, see Timasheff et al., 1992), may be reinvestigated.

Our fluorescent derivative of paclitaxel, however, appears to behave differently than DMAT. Initial fluorescence spectra we performed with 2-AB-PT in the presence of low tubulin concentrations showed emission maxima at ~430 nm, which is the maximum of 2-AB-PT bound to microtubules.

Electron micrographs of these samples, however, showed the presence of a few short microtubules (Han and Bane, unpublished data). When microtubules formed with 2-AB-PT were separated from unassembled protein by ultracentrifugation, the emission spectrum of the supernatant displayed a maximum near 453 nm, which is characteristic of unbound 2-AB-PT. Thus, under our experimental conditions, we found no evidence for 2-AB-PT binding to the unassembled tubulin dimer. The differences in our results and the results with DMAT may be related to the structures of the two paclitaxel analogs. The fluorophore on 2-AB-PT is clearly in a region on the taxane skeleton where minor modifications of the substituent can significantly affect the activity of the drug, while the fluorophore on DMAT is in a portion of the paclitaxel molecule in which wider structural variation can occur with minimal loss of activity (Kingston, 1991).

Although we did not find evidence of 2-AB-PT binding to dimeric tubulin, we did observe characteristic microtubule-bound fluorescence of 2-AB-PT in solutions in which low concentrations of tubulin were prebound to colchicine. No microtubules were observed by light scattering or in electron micrographs of these samples. These results were in agreement with a report by Carlier and Pantaloni (1983) that paclitaxel binds to the tubulin−colchicine complex. Carlier and Pantaloni monitored activation of the endogenous GTPase activity of tubulin−colchicine to detect paclitaxel binding, but did not investigate the aggregation state of the sample. We therefore rigorously characterized the aggregation state of tubulin−colchicine in the presence of 2-AB-PT under conditions in which characteristic tubulin-bound 2-AB-PT emission is observed. Our finding that the sole protein species in solution is 6S tubulin demonstrates that 2-AB-PT binds to $\alpha-\beta$ tubulin heterodimer in the form of the tubulin−colchicine complex. These data also serve to support Carlier and Pantaloni's original conclusion that paclitaxel binds to unpolymerized tubulin−colchicine.

Attempts were made to determine if the 2-AB-PT binding site on the tubulin−colchicine complex is the same as the paclitaxel binding site on microtubules. No displacement of 2-AB-PT bound to tubulin−colchicine by paclitaxel was observed at paclitaxel concentrations up to 10-fold that of 2-AB-PT. (Paclitaxel at these concentrations did not induce aggregation of tubulin−colchicine; Figure 10B.) Carlier and Pantaloni (1983) determined the K_d for paclitaxel binding to tubulin−colchicine to be 13 μM. If we assume this K_d value for both 2-AB-PT and paclitaxel binding to tubulin−colchicine at a single site, then the binding site would be about 20% occupied with 2-AB-PT and about 80% occupied with paclitaxel under the experimental conditions in which maximum binding of both drugs could be obtained. Thus, under the experimental conditions restricted by the solubilities of the two drugs, it is unlikely that competition between the two molecules for a single binding site would be observed. It is therefore unclear if the binding site for 2-AB-PT on tubulin−colchicine is distinct from the paclitaxel binding site on microtubules, or if displacement did not occur due to low affinity of the ligands for tubulin−colchicine.

It must also be noted that tubulin complexed to colchicine possesses a different conformation than the tubulin dimer (Hamel, 1990; Perez-Ramirez & Timasheff, 1994). The data presented above therefore cannot confirm a possible role of paclitaxel binding to heterodimer tubulin as a key step in the mechanism of paclitaxel-induced tubulin assembly. These data do support the idea, though, that the paclitaxel binding site on microtubules may be wholly contained on a single tubulin dimer, which is most likely located on the β-subunit of tubulin (Nogales et al., 1995; Rao et al., 1995).

CONCLUSIONS

The fluorescent paclitaxel derivative 2-AB-PT binds to the paclitaxel site on microtubules with an affinity only slightly less than paclitaxel itself. An additional, lower affinity site(s) for 2-AB-PT on microtubules also exists, but it is unclear if this second site is also shared with paclitaxel. A low affinity binding for 2-AB-PT to the tubulin−colchicine complex has also been observed, but the relationship between 2-AB-PT and paclitaxel binding to tubulin−colchicine is uncertain.

The paclitaxel binding site on microtubules has been characterized by steady-state absorption and fluorescence spectroscopy. The 2-benzoyl substitutent of paclitaxel is in contact with the protein when paclitaxel is bound to the microtubule. This region of the binding site is not purely hydrophobic, and it possesses a hydrogen bond donor in the vicinity of the *meta* position on the aromatic ring.

ACKNOWLEDGMENT

We thank Dr. Barbara M. Poliks and Mr. Henry Eichelberger for the electron microscopy work.

REFERENCES

Birmachu, W., & Reed, J. K. (1988) *Photochem. Photobiol. 47*, 675−683.
Caplow, M., Shanks, J., & Ruhlen, P. (1994) *J. Biol. Chem. 269*, 23399−23402.
Carlier, M.-F., & Pantaloni, D. (1983) *Biochemistry 22*, 4814−4822.
Chabin, R. M., Feliciano, F., & Hastie, S. B. (1990) *Biochemistry 29*, 1869−1875.
Chaudhary, A. G., Gharpure, M. M., Rimoldi, J. M., Chordia, M. D., Gunatilaka, A. A. L., Kingston, D. G. I., Grover, S., Lin, C. M., & Hamel, E. (1994) *J. Am. Chem. Soc. 116*, 4097−4098.
Chen, S.-H., Farina, V., Wei, J.-M., Long, B., Fairchild, C., Mamber, S. W., Kadow, J. F., Vyas, D., & Doyle, T. W. (1994) *Bioorg. Med. Chem. Lett. 4*, 479−482.
Cheung, H. (1991) in *Topics in Fluorescence Spectroscopy, Principles* (Lakowicz, J. R., Ed.) Vol. 2, pp 127−176, Plenum Press, New York.
Demas, J. N., & Crosby, G. A. (1971) *J. Phys. Chem. 75*, 991−1024.
Detrich, H. W., III, & Williams, R. C., Jr. (1978) *Biochemistry 17*, 3900−3907.
Dhamodharan, R., Jordan, M. A., Thrower, D., Wilson, L., & Wadsworth, P. (1995) *Mol. Biol. Cell. 6*, 1215−1229.
Diaz, J. F., & Andreu, J. M. (1993) *Biochemistry 32*, 2747−2755.
Dimroth, K., Reichardt, C., Seipmann, F., & Bohlmann, F. (1963) *Justus Liebigs Ann. Chem. 661*, 1−37.
Dubois, J., Guénard, D., Guéritte-Voegelein, F., Guedira, N., Potier, P., Gillet, B., & Beloeil., J.-C. (1993) *Tetrahedron 49*, 6533−6544.
Dubois, J., Le Goff, M.-T., Gueritte-Voegelein, F., Guenard, D., Tollon, Y., & Wright, M. (1995) *Bioorg. Med. Chem. 3*, 1357−1368.
Georg, G. I., Ali, S. M., Boge, T. C., Datta A., Falborg, L., Park, H., Mejillano, M., & Himes, R. H. (1995) *Bioorg. Med. Chem. Lett. 5*, 259−264.
Hamel, E. (1990) *Microtubule Proteins* (Avila, J., Ed.) pp 89−191, CRC Press, Boca Raton, FL.
Han, Y., Chaudhary, A. G., Chordia, M. D., Sackett, D. L., Kingston, D. G. I., & Hastie, S. B. (1994) *Mol. Biol. Cell* 5 (Suppl.), 285a.
Hastie, S. B. (1989) *Biochemistry 28*, 7753−7760.
Horwitz, S. B. (1992) *Trends Pharm. Sci. 13*, 134−136.

Kingston, D. G. I. (1991) *Pharmacol. Ther. 52*, 1−34.
Lakowicz, J. R. (1983) *Principles of Fluorescence Spectroscopy*, Plenum Press, New York.
Lippert, V. E. (1957) *Z. Electrochem. 61*, 962−975.
Mataga, N. (1963) *Bull. Chem. Soc. Jpn. 36*, 654−662.
Mataga, N., Kaifu, Y., & Kaizumi, M. (1956) *Bull. Chem. Soc. Jpn. 29*, 465−470.
Na, G. C., & Timasheff, S. N. (1980) *Biochemistry 19*, 1347−1354.
Na, G. C., & Timasheff, S. N. (1981) *J. Mol. Biol. 151*, 165−178.
Na, G. C., & Timasheff, S. N. (1982) *Methods Enzymol. 85*, 393−408.
Nogales, E., Wolf, S. G., Khan, I. A., Luduena, R. F., & Downing, K. H. (1995) *Nature 375*, 424−427.
Parness, J., & Horwitz, S. B. (1981) *J. Cell Biol. 91*, 479−487.
Penefsky, H. A. (1977) *J. Biol. Chem. 252*, 2891−2899.
Perez-Ramirez, B., & Timasheff, S. N. (1994) *Biochemistry 33*, 6262−6267.
Perez-Ramirez, B., Shearwin, K. E., & Timasheff, S. N. (1994) *Biochemistry 33*, 6253−6261.
Rao, S., Krauss, N. E., Heerding, J. M., Swindell, C. S., Ringel, I., Orr, G. A., & Horwitz, S. B. (1994) *J. Biol. Chem. 269*, 3132−3134.
Rao, S., Orr, G. A., Chaudhary, A. G., Kingston, D. G. I., & Horwitz, S. B. (1995) *J. Biol. Chem. 270*, 20235−20238.
Ringel, I., & Horwitz., S. B. (1991) *J. Pharmacol. Exp. Ther. 259*, 855−860.
Rowinski, E. K., Onetto, N., Canetta Renzo, M., & Arbuck, S. G. (1992) *Semin. Oncol. 19*, 646−662.
Sacket, D. L., & Lippoldt, R. E. (1991) *Biochemistry 30*, 3511−3517.
Sengupta, S., Boge, T. C., Georg, G. I., & Himes, R. H. (1995) *Biochemistry 34*, 11889−11894.
Shearwin, K. E., Perez-Ramirez, B., & Timasheff, S. N. (1994) *Biochemistry 33*, 885−893.
Shire, S. J., Holladay, L. A., & Rinderknecht, E. (1991) *Biochemistry 30*, 7703−7711.
Souto, A. A., Acuna, A. U., Andrea, J. M., Barasoain, I., Abal, M., & Amat-Guerri, F. (1995) *Angew. Chem., Int. Ed. Engl. 34*, 2710−2712.
Thulborn, K. R., & Sawyer, W. H. (1978) *Biochim. Biophys. Acta 511*, 125−140.
Timasheff, S. N., Andreu, J. M., & Na, G. C. (1991) *Pharmacol. Ther. 52*, 191−210.
Vander Velve, D. G., Georg, G. I., Grunewald, G. L., Gunn, C. W., & Mitscher, L. A. (1993) *J. Am. Chem. Soc. 115*, 11650−11651.
Williams, H. J., Scott, A. I., & Dieden, R. A. (1993) *Tetrahedron 49*, 6545−6560.
Williams, R. C., Jr., & Lee, J. C. (1982) *Methods Enzymol. 85*, 376−385.
Wilson, L., & Jordan, M. A. (1995) *Chem. Biol. 2*, 569−573.

BI960774L